Zubiaga, A.; Tuomisto, F.; Puska, M.J.

Matter-positronium interaction: An exact diagonalization study of the He atom - positronium system

Published in:
Physical Review A

DOI:
10.1103/PhysRevA.85.052707

Published: 01/05/2012

Document Version
Publisher's PDF, also known as Version of record

Please cite the original version:
Zubiaga, A., Tuomisto, F., & Puska, M. J. (2012). Matter-positronium interaction: An exact diagonalization study of the He atom - positronium system. *Physical Review A*, *85*(5), 1-7. [052707].
https://doi.org/10.1103/PhysRevA.85.052707

Matter-positronium interaction: A study of the He-atom–positronium system

A. Zubiaga,* F. Tuomisto, and M. J. Puska
Department of Applied Physics, Aalto University, P.O. Box 11100, FIN-00076 Aalto Espoo, Finland
(Received 29 February 2012; published 16 May 2012)

The many-body system comprising a He nucleus, three electrons, and a positron has been studied using an explicitly correlated Gaussians basis and a stochastic variational method for the optimization of the basis. The purpose has been to clarify to which extent the system can be considered as a distinguishable positronium (Ps) atom interacting with a He atom and, thereby, to pave the way to a practical atomistic modeling of Ps states and annihilation in matter. The maximum value of the distance between the positron and the nucleus is constrained and the Ps atom at different distances from the nucleus is identified from the electron and positron densities, as well as from the electron-positron distance and center-of-mass distributions. The polarization of the Ps atom increases as its distance from the nucleus decreases. The contact density of the electrons of He with the positron is depleted, particularly when the overlap is small. The ortho-Ps pick-off annihilation rate calculated as the overlap of the positron and the free He electron densities has to be corrected for the observed depletion, especially at large pores or voids.

DOI: 10.1103/PhysRevA.85.052707 PACS number(s): 34.80.Lx, 31.15.ac, 36.10.Dr

I. INTRODUCTION

The ortho-Positronium (o-Ps) atom is the bound state of an electron and a positron with the total spin $S = 1$. It is formed in molecular matter and in some insulators, such as SiO_2, because the electron density is low in the interstitial region unlike in metals or semiconductors [1]. In vacuum, o-Ps has a relatively long lifetime of 142 ns because its annihilation via the fast two-gamma channel is prohibited by the conservation of the angular momentum. Annihilation through the two-gamma channel with an electron of an opposite spin is possible when o-Ps interacts with matter. The resulting pick-off annihilation depends on the overlap of the o-Ps with the electron density of the matter and it can reduce the positron lifetime remarkably [2]. While in metals and semiconductors, the short-range screening of the positron by the electron cloud induces an enhancement of the electron density around the positron, for o-Ps in molecular matter the electron accompanying the positron hinders efficiently further screening by electrons in the matter. The pick-off annihilation rate remains smaller than in metals and semiconductors because the repulsive electron-electron interaction between the electrons in Ps and matter prevents larger values of the overlap.

The pick-off annihilation lifetime spectroscopy of o-Ps has a rather unique role as a method capable to study open volumes in soft or porous materials in which Ps is formed. Size and density distributions of nanometer-scale voids in polymers [3], porous SiO_2 [4,5], and biostructures [6,7] have been estimated by measuring the pick-off annihilation rate of o-Ps. However, in order to make a reliable quantitative analysis of the experimental results, one should be able to model o-Ps states and annihilation in these structures with predictive power.

In contrast to an atom where the nuclear degrees of freedom can, to a good approximation, be treated classically, both the electron and the positron in the Ps atom are light quantum-mechanical particles and the nonadiabatic correlation effects have to be taken into account. For positrons in dense materials, such as metals and semiconductors, a good starting point is a separate calculation of the quantum-mechanical state of a single positron [8]. In practice, this calculation is based on the results of many-body theories for a delocalized positron in a homogeneous electron gas. The nature of the Ps atom calls for a quantum-mechanical many-body calculation of the interacting electron-positron system in the Coulomb field of nuclei as an external static potential. In the case of materials systems, this is clearly beyond the present computer capacity. An attractive starting point for modeling Ps is to consider it as a distinguishable particle also when it is interacting closely with matter. This is in line with the view of a long-living o-Ps interacting with matter and annihilating through a pick-off process.

The above-mentioned model of the Ps atom interacting as a single particle with matter finds support also from experimental and theoretical studies of Ps scattering off atoms and light molecules. Recently, the scattering of Ps off noble gas atoms and light closed-shell molecules has been measured using a slow mono-energetic Ps beam [9] and it has been seen to be dominated by the repulsive electron-electron interaction at short distances. At long distances the van der Waals attraction may play a role, especially in interactions with molecules of high polarizability.

The positronium hydride (HPs) bound state has been observed experimentally by Schader *et al*. [10] and its binding energy has been estimated to be around 1.1 eV (0.04 hartree). The bound states of Ps with several small atoms have been studied theoretically using explicitly correlated Gaussians basis optimized using a stochastic variational method (ECG-SVM). The most carefully studied system is HPs [11–13], which has been found to form a bound state with a binding energy of 0.039 hartree, in good agreement with the experimental value. LiPs [11,14,15] and NaPs [11,15] systems have also been predicted to form bound states with binding energies of 0.0123 and 0.0084 hartree, respectively. The calculations show that at large distances the positron overlaps with an extra electron forming a free Ps-like cluster, while, when the positron density overlaps with that of the electrons inside the

*asier.zubiaga@aalto.fi

atom, the Ps-like character is lost. In the case of closed-shell noble gas atoms, the electron-electron Pauli repulsion adds to the Coulombic repulsion and the formation of atom-Ps bound states is prevented. Thus far, only a small number of different atoms have been considered in this kind of accurate calculation, but it has been already observed that the atoms able to trap Ps have high electron affinities and open-shell electronic structures [16]. Closed shell molecules with high polarizability may also trap a positronium atom due to their stronger van der Waals attractive interaction but, to our knowledge, they have not yet been studied.

Mitroy and Ivanov have studied the scattering of *o*-Ps off rare-gas atoms and alkali metal ions [17,18]. They determined the scattering lengths for wave vectors up to 0.5 a_0^{-1} corresponding to the Ps energy of ∼1.7 eV. Besides rare-gas atoms, also molecules have small electron affinities. They typically have HOMO-LUMO gaps of up to 1 hartree and their electrons are well localized in molecular orbitals. In polymers and biomolecular materials, the main cohesive interaction between the molecules is the van der Waals interaction and their molecular orbitals are not greatly affected. Individual molecules still show HOMO-LUMO gaps and the repulsive Pauli interaction between electrons in neighboring molecules plays a role. On the other hand, the van der Waals interaction between the molecules and Ps can also be strong, especially for molecules of high polarizability.

A model widely used to study Ps in small pores and voids (<2 nm) is that developed by Tao and Eldrup [19,20]. The semi-empirical model relates the Ps lifetime and the pore-void radius. Ps is considered as a single particle and the pore or void is modeled using a spherical, cubic, or elliptic infinite potential well. The electron density of the material enters the void and forms a layer of the thickness ΔR on its surface. The pick-off annihilation rate is calculated from the overlap of the positron density with the electron density of the material. The parameter of the model, ΔR, is not well known for all the materials and its chemical dependence cannot be described. In addition, the model assumes compact pores inside the material. The model has been extended to larger pores including the annihilation with excited particle-in-a-box states distributed according to the Boltzmann distribution at a finite temperature [21].

Schmitz and Müller-Plathe [22] introduced an atomistic model to describe Ps states and annihilation at voids in polymers. The potential landscape for Ps is based on the superposition of interactions between the Ps atom and individual atoms. These interactions, in turn, include the long-range van der Waals interaction based on the polarizabilities of the Ps atom and the atoms in the polymer and the short-range repulsion between the electron in the Ps atom and the electrons of the material. The latter interaction is described by fitting to experimental scattering cross sections. The Ps wave function corresponding to a given finite temperature is solved for by the path integral Monte-Carlo method and, thereafter, the pick-off annihilation rate is calculated as the overlap of the positron density with the electron density, which is also obtained as a superposition over the atoms.

Our final goal is the atomistic modeling of a Ps atom interacting with molecular materials so that the necessary approximations made and the model parameters chosen are based on *ab initio* results. Studying theoretically the HePs system will help to understand several aspects in the properties of Ps also in molecular solids and liquids. This is because in molecules, electrons are also in a closed shell configuration and a HOMO-LUMO gap sets the minimum energy necessary for an extra electron (of the Ps atom) to enter into the electron cloud of the molecule.

The similarities between molecules with HOMO-LUMO gaps and closed-shell noble gas atoms in mind, we have calculated the many-body wavefunction and the total energy of the unbound HePs system by using ECG-SVM. In order to study the interaction of a Ps and a He atom at finite distances, the mean distance of the positron from the nucleus has been constrained. As a result, a set of configurations has been considered with the nucleus-positron mean distance ranging between 1.87 and 47.67 a.u. Electron and positron densities, interaction energies, and annihilation rates have been calculated and analyzed in order to clarify to which extent the picture of the distinguishable Ps particle can be applied.

II. STOCHASTIC VARIATIONAL METHOD AND THE MODELING OF THE HePs SYSTEM

We have described the N-particle system comprising the heavy nucleus (treated as a single particle), light electrons, and the positron by the nonrelativistic Hamiltonian

$$\widehat{H} = \sum_i \frac{\vec{p}_i^{\,2}}{2m_i} - T_{\rm cm} + \sum_{i<j} \frac{q_i q_j}{4\pi\epsilon_0 r_{ij}}, \tag{1}$$

where $\vec{p}_i$, m_i, and q_i, are the momenta, masses, and charges of the particles, respectively, r_{ij} is the distance between the ith and jth particles, and $T_{\rm cm}$ is the center-of-mass (CM) kinetic energy. The wavefunction is written as a linear combination of properly antisymmetrized explicitly correlated Gaussian (ECG) [23] functions as

$$\begin{aligned}\Psi &= \sum_{i=1}^{s} c_i\ \psi^i_{SMs}(\vec{x}, A^i) \\ &= \sum_{i=1}^{s} c_i\ \mathcal{A}\left[\exp\left(-\frac{1}{2}\sum_{\mu,\nu=1}^{N-1} A^i_{\mu\nu}\vec{x}_\mu\vec{x}_\nu\right)\otimes\chi_{SMs}\right],\end{aligned} \tag{2}$$

where $\mathcal{A}$ is an antisymmetrization operator and χ_{SMs} is the spin eigenfunction with $\hat{S}^2\chi_{SMs} = S(S+1)\hbar^2\chi_{SMs}$ and $\hat{S}_z\chi_{SMs} = M_S\hbar\chi_{SMs}$. We have considered only the spherically symmetric total angular momentum $L = 0$ states. The mixing coefficients c_i are obtained by diagonalizing the Hamiltonian matrix $\langle\psi^i_{SMs}|\widehat{H}|\psi^j_{SMs}\rangle$. The nonlinear coefficients $A^i_{\mu\nu}$ are randomly generated and a new $A^i_{\mu\nu}$ is kept only if the update lowers the total energy of the system. Using the Jacobi coordinate set $\{\vec{x}_1,\ldots,\vec{x}_{N-1}\}$, with the reduced mass of the ith coordinate as $\mu_i = m_{i+1}\frac{\sum_{i=1}^{i} m_i}{\sum_{i=1}^{i+1} m_i}$, allows for a straightforward separation of the CM movement and, therefore, the total number of "particles" treated is $N-1$.

The stochastic variational method is suitable for calculating many-body wavefunctions, such as Ψ in Eq. (2), for small systems [23]. The number of particles is limited by the present algorithms and computer capacity typically to less than seven

particles. The ECG basis comprises in our calculations 600 functions. The matrix elements between the basis functions are computed analytically in an efficient manner. In order to keep the size of the ECG basis small, the basis set is optimized by choosing the most appropriate nonlinear parameters $A^i_{\mu\nu}$ for the Gaussian functions using a stochastic search in the parameter space. The large number of parameters to optimize, up to tens of thousands, prevents the use of direct search methods. The best nonlinear parameter for each pair is chosen after 25 trials within each optimization cycle and 20 optimization cycles are done for each basis function. The trial values are obtained choosing values between a certain minimum and maximum using a random number generator.

SVM can be also used to study unbound systems setting boundaries to the possible values of the nonlinear parameters $A^i_{\mu\nu}$; i.e., increasing the minimum value the particles can be prevented to separate to the infinity [17]. The configurations with the lowest energy are searched for within the available parameter space, i.e., the energy is minimized within a constrained parameter space. In order to model the interaction between He and the Ps atom at different distances it is enough to set a constraint only to the nonlinear parameter $A^i_{\mu\nu}$ corresponding to the nucleus-positron pair. Thus, the size of the parameter space available for optimizing the wavefunction is not seriously restricted. The nucleus-positron distance parameter $l_{\mathrm{He}-p}$ corresponding to the maximum of the nonlinear parameter, $A^i_{\mathrm{He}-p} = (1/l^i_{\mathrm{He}-p})^2$, is varied between 1 and 50 a.u. The wavefunction and the total energy of the HePs system are then calculated for each constrained He-Ps distance. Due to practical reasons, the nucleus-electron distance parameter $l_{\mathrm{He}-e}$ also has to be limited. We have checked that using $l^i_{\mathrm{He}-e} \leqslant 200$ a.u. gives structures and energies well-enough converged for our discussion below. On the other hand, the lower limit is set equal to 0.0001 a.u. in all cases to avoid unphysical Dirac-delta-like wavefunctions.

The kinetic energy ($\langle T\rangle$) and the potential energy ($\langle V\rangle$) of a system interacting through Coulomb potentials are related by the Virial theorem $2\langle T\rangle = -\langle V\rangle$. Any deviation from this relation is due to an inadequate basis function set. Optimizing the basis set the virial coefficient $(\frac{2\langle T\rangle}{\langle V\rangle} + 1)$ decreases in magnitude.

In order to study the many-body wavefunction of the system, the positron $[\rho_p(r) = \langle\Psi|\delta(\vec{r}_p - \vec{r}_N - \vec{r})|\Psi\rangle]$ and electron $[\rho_e(r) = \sum_{i=1}^{N_e}\langle\Psi|\delta(\vec{r}_{i,e} - \vec{r}_N - \vec{r})|\Psi\rangle]$ density distributions are plotted. Above, $\vec{r}_N$ is the position vector of the nucleus and the index i runs over all the electrons N_e. The e-p pair correlation function is calculated as

$$\rho_{e-p}(\vec{r}) = \sum_{i=1}^{N_e}\langle\Psi|\delta(\vec{r}_i - \vec{r}_p - \vec{r})|\Psi\rangle. \tag{3}$$

The distribution of the electron-positron (e-p) CM is defined as

$$\rho^{\mathrm{CM}}_{e-p}(\vec{r}) = \sum_{i=1}^{N_e}\langle\Psi|\delta\big(\vec{r}^{\,\mathrm{CM}}_i - \vec{r}\big)|\Psi\rangle, \tag{4}$$

where $\vec{r}^{\,\mathrm{CM}}_i = (\vec{r}_{i,e} + \vec{r}_p)/2$ is the center of mass of the positron and the ith electron and i runs over all the N_e electrons in the HePs system. The calculated distributions do not have any angular dependency and the radial distributions are the solid-angle-averaged distributions multiplied by the radius squared.

The two electrons of the He atom are prepared in the $S = 0$ state while the electron and the positron of the o-Ps are in the $S = 1$ state. The total spin angular momentum of the system is, then, $S = 1$. For the pick-off annihilation rate Γ^{po}, the $S = 0$ component of the ith electron-positron pair is selected through the $\widehat{P}^{i-p}_{S=0}$ spin projector, i.e.,

$$\Gamma^{\mathrm{po}} = 4\pi r_0^2 c\sum_{i=1}^{N_e}\langle\Psi|\delta(\vec{r}_i - \vec{r}_p)\widehat{P}^{i-p}_{S=0}|\Psi\rangle, \tag{5}$$

where r_0 is the classical electron radius and c is the speed of light. The summation runs over all the N_e electrons.

III. RESULTS & DISCUSSION

Before discussing the main topic of this work—the identification of the Ps atom within the HePs system—we will consider the energetics of the HePs system. The interaction energy E_I of HePs is defined as the difference between the total energy of the interacting system and the sum of the energies E_{He} and E_{Ps} of the isolated He and Ps atoms, respectively, i.e., $E_I = E_{\mathrm{HePs}} - E_{\mathrm{He}} - E_{\mathrm{Ps}}$. $E_{\mathrm{Ps}} = -0.24999999999$ hartree and $E_{\mathrm{He}} = -2.903693749$ Ha have been obtained from SVM calculations with a basis of 56 functions (virial coefficient $= 3.0 \times 10^{-11}$) and 600 functions (virial coefficient $= 1.8\times10^{-10}$), respectively. The interaction energy is shown in Fig. 1 as a function of the nucleus-positron mean distance $\langle r_p\rangle$. E_I is positive and approaches zero for large $\langle r_p\rangle$ values. For $\langle r_p\rangle$ smaller than 2.5 a.u., E_I is larger than E_{Ps}. Our calculations do not show the formation of the bound He-e$^+$ system. He can bind a positron only when it is in the $S = 3$ state [24] and its energy is 0.4 hartree above the highest energy we have considered for the HePs system. It

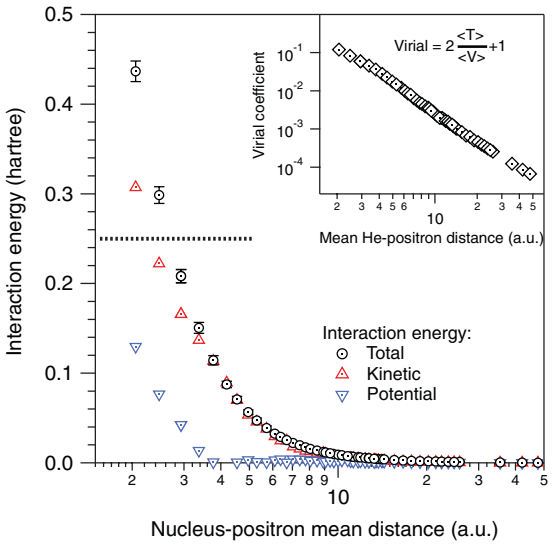

FIG. 1. (Color online) Total interaction energy (black circles) and its kinetic (red up-pointing triangle) and potential (blue down-pointing triangle) energy contributions as a function of $\langle r_p\rangle$. The horizontal dotted line denotes the energy above which the Ps atom is unstable against dissociation. The inset shows the log-log plot of the virial coefficient versus $\langle r_p\rangle$.

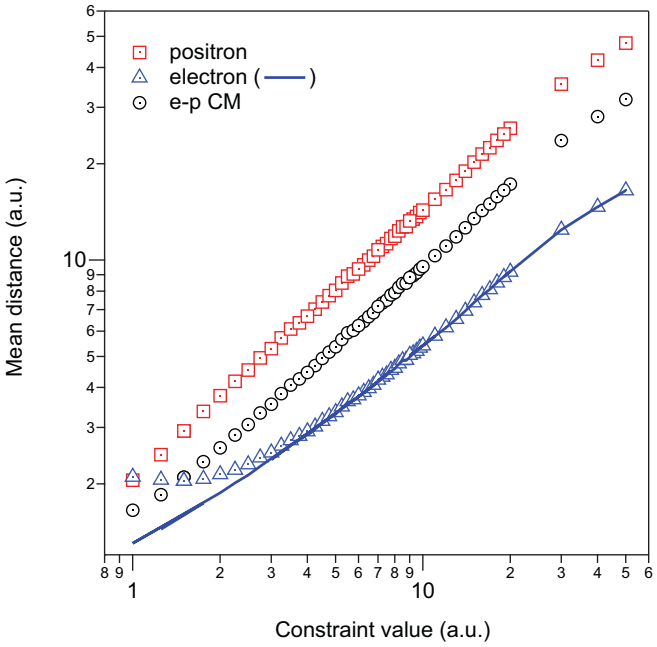

FIG. 2. (Color online) Positron (red squares), electron (blue triangles), and electron-positron CM (black circles) mean distances from the He nucleus for different calculated configurations versus the nucleus-positron distance parameter $l_{\mathrm{He}-p}$. The electron mean distance (blue line) obtained from the unpolarized Ps model is also given.

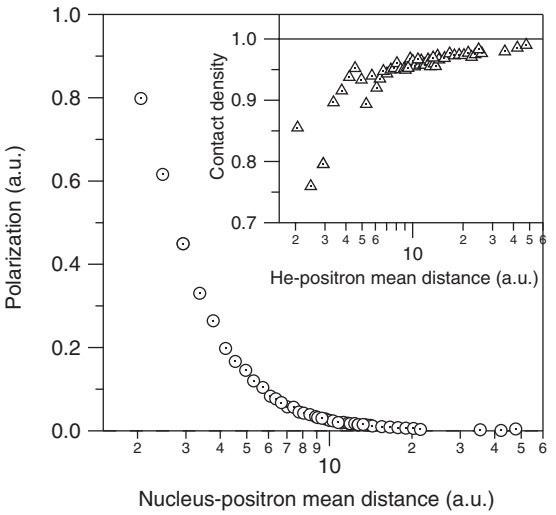

FIG. 3. The polarization parameter for all the calculated HePs configurations as a function of the positron mean distance $\langle r_p \rangle$ from the He nucleus. The inset shows the electron-positron contact density corresponding to the Ps atom component as a function of $\langle r_p \rangle$. The solid line indicates the contact density of free Ps.

should be noticed that, already at 5 a.u., the interaction energy is clearly above the energy of a thermalized Ps.

The error of the interaction energy ΔE has been estimated as the total energy decrease after an optimization loop of the function basis. For the optimization loop the best nonlinear parameter has been chosen for each pair after 25 trials. This procedure has been repeated 20 times for each basis function. For the most confined systems, $\langle r_p \rangle = 2$ a.u., $\Delta E = 0.01$ hartree and the virial coefficient is $\sim$0.1. The confinement method shrinks the parameter space available to optimize the basis. In addition, the many-body wavefunction has to include the strong correlations happening in confined systems. Accordingly, the convergence is slow and the virial coefficient is large. For $\langle r_p \rangle = 48$ a.u., the error and the virial coefficient decrease to $\Delta E = 2 \times 10^{-5}$ and 7×10^{-5} hartree, respectively.

Figure 1 also shows the decomposition of the interaction energy to the kinetic and potential energy contributions. They are defined similarly to the total interaction energy. E_{Kin} is the main contribution to the interaction energy at distances shorter than 10 a.u., mostly due to the confinement of Ps and its small mass. E_{Pot} is always positive and at very short distances (<4 a.u.) it grows very fast.

The calculated mean distances of electrons $\langle r_e \rangle$, the positron $\langle r_p \rangle$, and the electron-positron CM $\langle r_{e-p}^{\mathrm{CM}} \rangle$ from the He nucleus are shown in Fig. 2 as a function of the nucleus-positron distance parameter $l_{\mathrm{He}-p}$ corresponding to the confinement of the system. The mean distances grow monotonically because HePs is ultimately unbound and, as expected when a Ps atom is formed, $\langle r_e \rangle$ increases following $\langle r_p \rangle$. At $l_{\mathrm{He}-p} < 5$ a.u., $\langle r_e \rangle$ saturates to a value of 2 a.u. because the electron of Ps does not penetrate into the He core. On the average, it stays at $\sim$4 a.u. from the nucleus (see Fig. 4). On the other hand, $\langle r_{e-p}^{\mathrm{CM}} \rangle$ continues to decrease because the positron keeps being confined.

Using $\langle r_p \rangle$ and assuming that the Ps atom is not polarized, $\langle r_e \rangle$ can be approximated [25] as the sum of two-thirds of the mean electron distance in the He atom of 0.93 a.u. and one-third of the mean positron distance $\langle r_p \rangle$ (blue line in Fig. 2). The agreement with the $\langle r_e \rangle$ calculated from the many-body wavefunction is very good when $\langle r_p \rangle$ is larger than 7–8 a.u. (or the nucleus-positron distance parameter $l_{\mathrm{He}-p}$ is larger than 4–5 a.u.). For smaller $l_{\mathrm{He}-p}$ values the actual $\langle r_e \rangle$ is larger than the estimated one, which reflects the polarization of the Ps atom when approaching the He nucleus. The difference can actually be taken as a measure of the polarization (see Fig. 3). For $\langle r_p \rangle = 20$ a.u. the polarization parameter is very small ($\sim 6 \times 10^{-3}$ a.u.). The polarization starts to increase when $\langle r_p \rangle$ is below 10 a.u., and at 4 a.u. its value is $\sim$0.2 a.u., i.e., 10% of the electron-positron mean distance for an isolated Ps. The maximum value of the polarization parameter is 0.8 a.u. when the interaction energy is 0.44 hartree and Ps is actually unstable against dissociation. According to our calculations, the smallest stable configuration corresponds to $\langle r_p \rangle \sim 2.9$ a.u. and a polarization parameter of $\sim$0.45 a.u.

The electron-positron contact density of the Ps atom (shown in the inset of Fig. 3) has been obtained by subtracting the contribution of the He electrons estimated as two times the electron-positron contact density of the $S = 0$ electron-positron pair. At $\langle r_p \rangle = 20$ a.u., the contact density within the Ps atom reaches the value of 0.97, which is close to the exact value of 1 for an isolated Ps. At $\langle r_p \rangle = 4$ a.u. the contact density is still $\sim$0.94 and at the smallest separation decreases down to 0.76. The decrease of the contact density reflects increasing polarization of the Ps atom in the interaction with the He atom.

Figure 4 shows the radial distributions of the positron and the electrons in HePs configurations corresponding to the

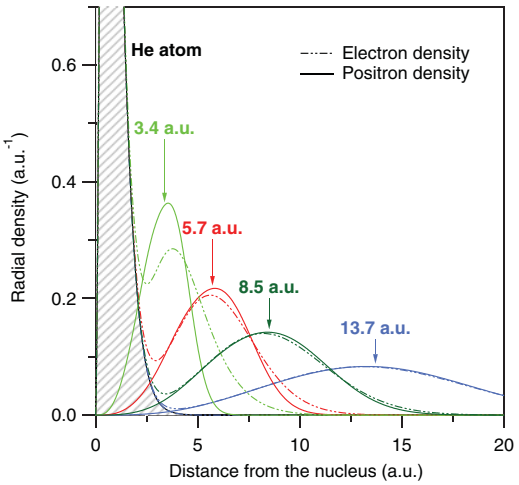

FIG. 4. (Color online) Radial distributions of the positron (full lines) and electrons (dashed lines) for four different configurations of the HePs system with $\langle r_p \rangle$ values of 3.4 a.u. (light green), 5.7 a.u. (red), 8.5 a.u. (dark green), and 13.7 a.u. (blue). The arrowed tags indicate the position and the value of the positron mean distances $\langle r_p \rangle$ from the He nucleus for each configuration. The shading gives the electron density of a free He atom. All the distributions are normalized to the total number of particles.

positron mean distance $\langle r_p \rangle$ ranging from 3.4 to 13.7 a.u. The electron distribution can be decomposed into two components. The larger corresponds closely to the undisturbed electron density of a He atom. The second maximum overlaps with the positron distribution especially well for large $\langle r_p \rangle$, indicating the formation of a well-distinguishable Ps atom. At small separations, the overlap of the electron and positron distributions weakens, indicating the increase of the polarization of the Ps atom.

Figure 5 shows the radial electron-positron correlation distribution of four HePs configurations and for the isolated Ps atom. The distribution is calculated from Eq. (3) and it is normalized to the total number of electrons. When $\langle r_p \rangle = 3.4$ a.u., the electron-positron pair correlation function shows a single peak, but when $\langle r_p \rangle$ is 5.7 a.u. a second peak appears as a shoulder, at 2 a.u. It corresponds to the electron-positron pair correlation function inside the Ps atom and when $\langle r_p \rangle$ is larger it converges to the electron-positron pair correlation of an isolated Ps atom. The other peak follows the positron distribution when it recedes from the He nucleus and it corresponds to the correlation between the positron and the electrons of the He atom. However, even at 8.5 a.u., the interaction between He and Ps affects the electron-positron correlations and the appearance of the Ps atom is not so clear-cut as in the electron distribution in Fig. 4.

The distribution of the *e-p* CM, shown in Fig. 6, can also be decomposed into two components. The larger component is closer to the He nucleus and its integrated intensity is double that of the smaller and more delocalized component. Thus, the larger and the smaller components correspond to the two electrons of the He atom and the electron of the Ps atom, respectively. The Ps component is very similar to the positron radial density, especially when the mean He nucleus-positron distance is larger than 5 a.u.

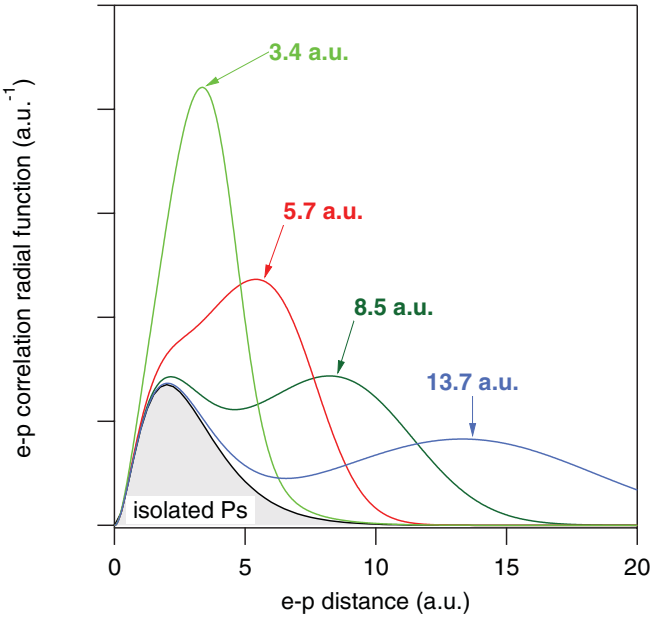

FIG. 5. (Color online) Electron-positron pair correlation function for the four HePs configurations described in the legend of Fig. 4. The arrowed tags show the corresponding $\langle r_p \rangle$ of each curve. The correlation distance for the isolated Ps atom (filled curve) is shown for comparison. All the electron-positron correlation curves are normalized to the number of electrons in the system in question.

Figure 7 shows the positron pick-off annihilation rate Γ^{po} as a function of $\langle r_p \rangle$, calculated using Eq. (5). It is an important magnitude for understanding Ps lifetime experiments in

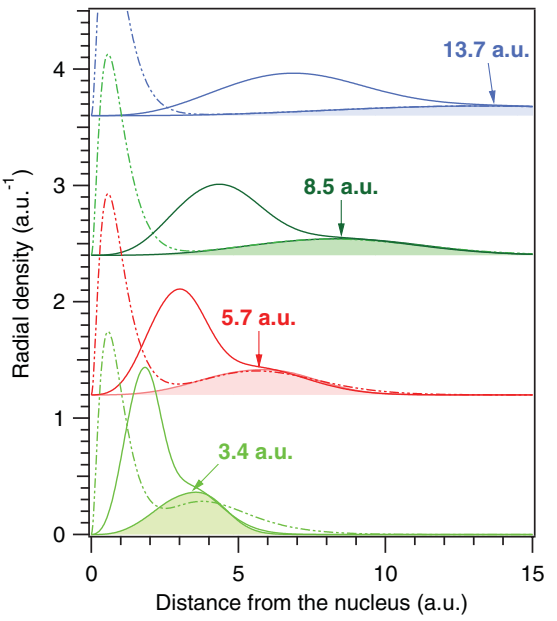

FIG. 6. (Color online) Electron-positron CM distribution for the four HePs configurations described in the legend of Fig. 1. The curves of each configuration have been separated vertically for better visibility. The arrowed tags show the corresponding $\langle r_p \rangle$ of each curve. The electron (dashed) and the positron (filled areas) radial distributions are also shown for comparison. The CM distributions are normalized to the number of electrons.

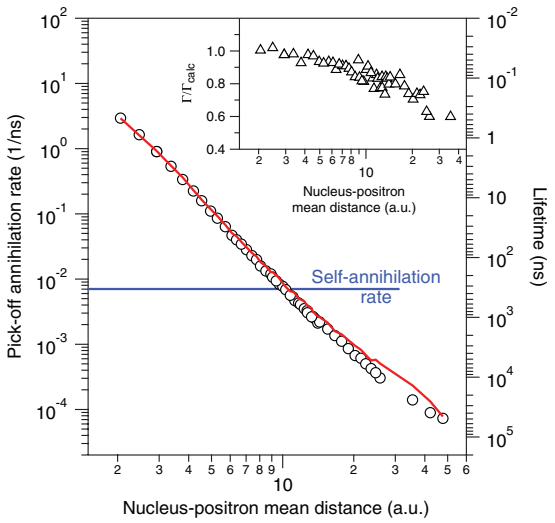

FIG. 7. (Color online) Positron annihilation rate obtained from the SVM results using Eq. (5) (black circles) and from the overlap of the free He atom and the positron densities, using Eq. (6) (solid red line). The inset shows the ratio of the values. The blue horizontal line gives the self-annihilation rate of o-Ps.

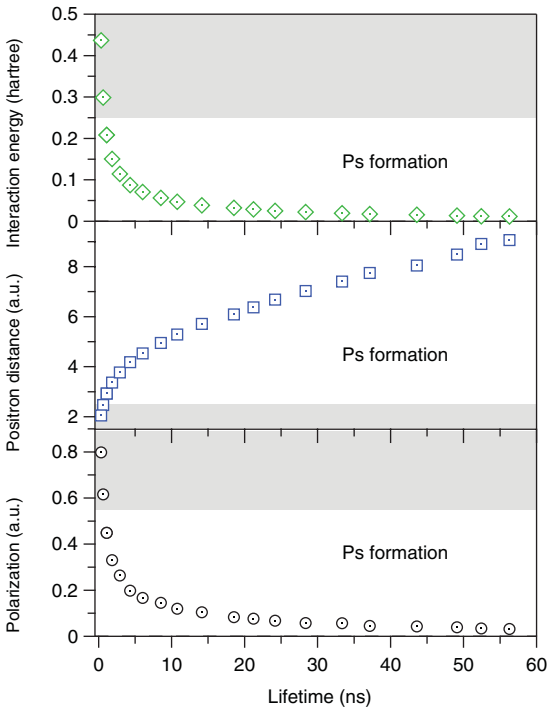

FIG. 8. (Color online) The polarization (black circles), the He nucleus-positron distance (blue squares), and the interaction energy (green diamonds) of the HePs system as a function of the positron lifetime. The grey area indicates the value range where the interaction energy of Ps atom is larger than its binding energy.

molecular matter and it also reflects the interaction of the Ps and He atoms and its behavior. The projector $\widehat{P}^{i-p}_{S=0}$ in Eq. (5) ensures that the pick-off processes occur only with the He electron forming a spin-singlet state with the positron. $\Gamma^{\rm po}$ increases with the increasing overlap of the positron and He electron density. At $\langle r_p\rangle = 10$ a.u., $\Gamma^{\rm po}$ is about the same as the self-annihilation rate $\sim 7.04\times 10^{-3}$ 1/ns of o-Ps (lifetime $\tau \sim$ 142 ns). At 4 a.u., $\Gamma^{\rm po} \sim 0.2$ 1/ns ($\tau \sim 4.8$ ns) and for $\langle r_p\rangle \sim$ 2.5 a.u., $\Gamma^{\rm po}$ equals to 2 1/ns ($\tau = 500$ ps), the spin-averaged annihilation rate of Ps.

A nonselfconsistent positron pick-off annihilation rate is obtained from the overlap of the free He electron density $n^{\rm He}_{e^-}$ and the SVM positron density n_{e^+} as

$$\Gamma^{\rm po}_{\rm ov} = 4\pi r_0^2 c \int d\vec{r}\ \frac{1}{2} n^{\rm He}_{e^-}(\vec{r})\, n_{e^+}(\vec{r}). \qquad (6)$$

The free He electron density is from a SVM calculation and the factor one half reflects that only one electron in He annihilates with the positron. $\Gamma^{\rm po}_{\rm ov}$ is widely used to calculate the pick-off annihilation rate of o-Ps [26]. With increasing nucleus-positron mean distance, it agrees with the many-body $\Gamma^{\rm po}$ result until $\langle r_p\rangle \sim 5$ a.u. (solid line in Fig. 7). When $\langle r_p\rangle$ further increases, $\Gamma^{\rm po}_{\rm ov}$ remains higher than $\Gamma^{\rm po}$. The ratio $\Gamma^{\rm po}/\Gamma^{\rm po}_{\rm ov}$, shown in the inset of Fig. 7, ranges between 1 and 0.6. The most confined systems show the largest ratios and it decreases steadily until $\langle r_p\rangle \sim 30$ a.u. At the level of the o-Ps self-annihilation rate, the overlap of the annihilating positron with the He electrons has decreased by 20% compared to the undistorted He electron density. It should be noted that at large separations the overlap and the annihilation rate are very small, which is also reflected in the scatter of the overlap ratios.

In contrast to a positron in an electron gas, where the positron-electron contact density is enhanced [8], for Ps interacting with He the many-body effects induce a depletion of the contact density. The electron in Ps screens the charge of the positron and the electron-electron repulsion further decreases the contact density at the positron position, especially at low electron density values. Thus, in strongly confined systems, the contact density is relatively weakly affected, but in weak confinement it is strongly depleted. $\Gamma^{\rm po}_{\rm ov}$ needs to be corrected for this effect especially when calculating the annihilation rate in large voids or pores, where the contact density is small and the annihilation rate is largely overestimated.

Figure 8 summarizes the polarization parameter, He nucleus-positron mean distance, and the interaction energy of the HePs system as a function of the positron lifetime ($1/\tau = \Gamma^{\rm po} + 1/142.05$). The gray area marks where the interaction energy of Ps is larger than the Ps binding energy. The figure gives a clear idea about the magnitude of these quantities in different conditions.

IV. CONCLUSIONS

We have been interested in to what extent a separate Ps atom can be distinguished in a close interaction with a He atom, i.e., when the volume of the HePs system is constrained. According to our many-body calculations, the behavior of several measures, i.e., those of electron and positron mean distances from the He nucleus, electron, and positron densities, as well as electron-positron pair correlation function and center-of-mass distribution show the formation of a Ps atom that is weakly polarized until the mean He nucleus-positron mean distance $\langle r_p\rangle$ is shorter than $\sim$5 a.u. At shorter distances, the Ps atom also forms but it is strongly polarized. The most clear-cut evidence is given, simply, by the electron and positron densities shown Fig. 4. There, the electron density can be

decomposed into the He and Ps atom components and the positron density overlaps well with the electron density. Even at $\langle r_p \rangle \approx 5$ a.u. the positron-electron contact density is still high, ∼93% of that in the free Ps atom, and the polarization parameter indicating the imbalance of the electron and positron densities in the Ps atom is small, 0.2 a.u.

The above notions for the HePs system, generalized to molecules, supports the possibility of using a practical single-particle description for *o*-Ps in molecular materials. Many-body calculations could be used to define pairwise atom-Ps potentials, which could form the basis for the calculation of the Ps energy landscape in the material and obtain, subsequently, its distribution and pick-off annihilation lifetime. In that respect, the above-mentioned findings about the relative depletion of the contact density will simplify the reliable estimation of the pick-off annihilation rate.

ACKNOWLEDGMENTS

This work was supported by the Academy of Finland through individual fellowships and the center of excellence program. Thanks are due to K. Varga for providing us his ECG-SVM code. We also thank I. Makkonen, J. Mitroy, and T. Rantala for helpful discussions.

[1] S. V. Stepanov and V. M. Byakov, in *Principles and Application of Positron & Positronium Chemistry*, edited by Y. C. Jean, P. E. Mallon, and D. M. Schrader (World Scientific, Singapore, 2003), p. 117.

[2] O. E. Mogensen, in *Positron Annihilation in Chemistry*, edited by H. K. V. Lotsch (Springer-Verlag, Berlin, 1995), Vol. 58, p. 193.

[3] A. Uedono, R. Suzuki, T. Ohdaira, T. Uozumi, M. Ban, M. Kyoto, S. Tanigawa, and T. Mikado, J. Polym. Sci., Part B **36**, 2597 (1998).

[4] Y. Nagai, Y. Nagashima, and T. Hyodo, Phys. Rev. B **60**, 7677 (1999).

[5] L. Liszkay, C. Corbel, P. Perez, P. Desgardin, M.-F. Barthe, T. Ohdaira, R. Suzuki, P. Crivelli, U. Gendotti, A. Rubbia, M. Etienne, and A. Walcarius, Appl. Phys. Lett. **92**, 063114 (2008).

[6] P. Sane, E. Salonen, E. Falck, J. Repakova, F. Tuomisto, J. Holopainen, and I. Vattulainen, J. Phys. Chem. B letters **113**, 1810 (2009).

[7] A. W. Dong, C. Pascual-Izarra, S. J. Pas, A. J. Hill, B. J. Boyd, and C. J. Drummond, J. Phys. Chem. B **113**, 84 (2009).

[8] M. J. Puska and R. M. Nieminen, Rev. Mod. Phys. **66**, 841 (1994).

[9] S. J. Brawley, S. Armitage, J. Beale, D. Leslie, A. Williams, and G. Laricchia, Science **330**, 789 (2010).

[10] D. M. Schrader, F. M. Jacobsen, N.-P. Frandsen, and U. Mikkelsen, Phys. Rev. Lett. **69**, 57 (1992).

[11] G. G. Ryzhikh, J. Mitroy, and K. Varga, J. Phys. B: At. Mol. Opt. Phys. **31**, 3965 (1998).

[12] J. Mitroy, Phys. Rev. A **73**, 054502 (2006).

[13] S. Bubin and K. Varga, Phys. Rev. A **84**, 012509 (2011).

[14] J. Mitroy, J. At. Mol. Sci. **1**, 275 (2010).

[15] J. Mitroy and G. G. Ryzhikh, J. Phys. B: At. Mol. Opt. Phys. **34**, 2001 (2001).

[16] J. Mitroy, M. W. J. Bromley, and G. G. Ryzhikh, J. Phys. B: At. Mol. Opt. Phys. **35**, R81 (2002).

[17] J. Mitroy and I. A. Ivanov, Phys. Rev. A **65**, 012509 (2001).

[18] J. Mitroy, J. Y. Zhang, and K. Varga, Phys. Rev. Lett. **101**, 123201 (2008).

[19] S. J. Tao, J. Chem. Phys. **56**, 5499 (1972).

[20] M. Eldrup, D. Lightbody, and J. N. Sherwood, Chem. Phys. **63**, 51 (1981).

[21] T. L. Dull, W. E. Frieze, D. W. Gidley, J. N. Sun, and A. F. Yee, J. Phys. Chem. B **105**, 4657 (2001).

[22] H. Schmitz and F. Müller-Plathe, J. Chem. Phys. **112**, 1040 (2000).

[23] K. Varga and Y. Suzuki, Phys. Rev. C **52**, 2885 (1995).

[24] J. Mitroy, Phys. Rev. A **72**, 032503 (2005).

[25] A. Zubiaga, F. Tuomisto, and M. Puska, "Study of unbound HePs using exact diagonalization technique", in Material Science Forum (Trans. Tech. Publications, to be published).

[26] W. Brandt, S. Berko, and W. W. Walker, Phys. Rev. **120**, 1289 (1960).